Polymeric layer-by-layer microcapsules containing iron oxide magnetic nanoparticles exposed to breast cancer cells: A viability study using tetrazolium-based (MTT) and calcein-AM assays (LIVE-DEAD)

ROBERT POWELL[1], RUSSELL SWIFT[2], ADAM ASHCROFT[3], MEGAN ASHCROFT[3], KASIE BUSSARD[4], EVELYN EDEN[5], JOSE GADEA[5], VARUN JALAPATI[6], JORDAN JONCAS[7], KAHNEEF MARTIN[8] , RACHEL CHANSONG KANG[9], TIK SUNG[5], CELINA YU[5], NEDA HABIBI[1]*

[1]*Department of Biomedical Engineering, University of North Texas, Texas, USA.*
[2]*California Institute of Technology, California, USA*
[3]*Palos Verdes High School, California, USA*
[4]*Salt Lake Community College, Utah, USA*
[5]*Pasadena City Community College, California, USA*
[6]*Texas Academy of Math & Science (TAMS), University of North Texas, Texas, USA*
[7]*Bossier Parish Community College, Louisiana, USA*
[8]*Community College of Philadelphia, Pennsylvania, USA*
[9]*John Champe High School, Virginia, USA*
**neda.habibi@unt.edu*

Abstract: The Layer-by-Layer capsules combined with nanoparticles are emerging as promising and secure vehicles for drug delivery. The integration of nanoparticles introduces intelligent functionalities, particularly in targeted therapy. This investigation focused on assessing the impact of drug carriers on the viability of MDA-MB-231 breast cancer cells. Specifically, polymeric capsules were synthesized using a Layer-by-Layer approach, incorporating iron oxide magnetic nanoparticles. The Layer-by-Layer method involved constructing six bilayers of PAH/PSS on a $CaCO_3$ template, with iron oxide magnetic nanoparticles (MNPs) interspersed between the layers. The core was removed by applying the chelating agenlt EDTA, resulting in the fabrication of hollow capsules. Characterization of the capsules was performed using SEM and bright-field microscopy. Successful synthesis was confirmed as capsules/MNPs responded to an external magnetic field. Various concentrations of capsules/MNPs were introduced to cells, and cell viability was assessed using the tetrazolium-based MTT assay for quantitative measurements and the calcein-AM assay (Live-dead) for real-time visualization of live and dead cells. The findings revealed that adding 20 µl of capsule suspension (containing 14,000 capsules) to 100 µl of cell culture suspension preserved 90% cell viability. This study implies a feasible concentration of capsules for delivering compounds to cancer cells without inducing toxicity to normal cells.

Keywords: Layer-by-Layer, microcapsule, magnetic nanoparticle, viability, breast cancer

Introduction

Nanomedicine encompasses a diverse array of technologies designed to diagnose, treat, monitor, and control biological systems. It spans the medical applications of nanomaterials to the development of nanoelectronic biosensors and explores potential future applications of molecular nanotechnology [1]. At the forefront of this interdisciplinary field, significant attention is devoted to research on the intelligent delivery and precise targeting of therapeutic and diagnostic agents. Current challenges in chemotherapy, such as issues related to non-specific targeting, aqueous solubility, multidrug resistance, and limited specificity, stem from the systemic distribution of chemotherapeutic agents, leading to side effects caused by the drugs affecting both target and non-target cells [2]. Consequently, nanoparticles, designed as targeted carriers for drugs, are actively under development as non-biological alternatives to overcome the challenges associated with conventional drug delivery [3]. The benefits of encapsulating drugs in a carrier are less cytotoxicity to normal cells and prompting a triggered release only at the tumor site.

Magnetic nanoparticles (MNPs), ranging in size from 1 to 100 nm, exhibit remarkable promise in the realm of drug delivery owing to their inherent biocompatibility [4]. Their unique ability to be externally manipulated through magnetic fields enables precise control, making them a versatile tool for targeted therapies in diseases like cancer [5,6]. MNPs offer advantages such as reduced toxicity, enhanced stability, and superior permeability compared to alternative nanoparticles [5]. MNPs have been incorporated into other drug delivery systems, such as Layer microcapsules, to develop targeted systems [6,7].

Microcapsules created using the Layer-by-Layer (LbL) [8] technology represent microcapsules employed in drug delivery due to their straightforward fabrication process [9], biocompatibility, and impressive drug-loading capabilities [10-12]. In this approach, alternate absorption of opposite-charged polymers on a microsphere [10] followed by removing the core will result in hollow capsules with multilayered nanoshells [13]. These LbL capsules are constructed with polyelectrolyte bilayers, utilizing biodegradable materials like collagen (COL), hyaluronic acid (HA) [14], and poly-L-arginine (pARG) [7, 12, 15], as well as synthetic non-biodegradable materials such as poly(allylamine hydrochloride) (PAH) and poly(sodium 4-styrenesulfonate) (PSS) [15]. The unique properties of these capsules are that their multilayered nanoshell can incorporate nanoparticles. Past research has involved the adornment of LbL microcapsules with iron oxide magnetic nanoparticles, demonstrating a strategic approach to achieve smart [16-17] and targeted drug delivery [18-20].

While the clinical applications of microcapsules containing iron oxide magnetic nanoparticles hold promise, the comprehensive exploration of their interaction with cancer cells remains incomplete [2, 11, 21]. This study aims to fill this gap by examining the interaction between magnetic nanoparticles and LbL capsules with breast cancer cells, focusing on cell viability. The assessment involved utilizing Tetrazolium-based (MTT) [22] and Calcein-AM assays, both serving distinct functions in evaluating cell viability [23]. The MTT (3-(4,5-dimethylthiazol-2-yl)-2,5-diphenyltetrazolium bromide) assay measures cellular metabolic activity by employing a yellow tetrazolium salt [22]. This salt is reduced by mitochondrial dehydrogenases in metabolically active cells, forming purple formazan crystals. The MTT assay offers a quantitative evaluation of cell viability based on the produced formazan. On the other hand, the Calcein-AM (acetoxymethyl ester) assay assesses intracellular esterase activity. Calcein-AM is initially a non-fluorescent, cell-permeant dye that, when cleaved by esterases in live cells, generates green, fluorescent calcein [23]. This dye effectively distinguishes live cells (exhibiting green fluorescence) from dead cells, as it is cleaved and retained exclusively in viable cells. The assay enables real-time imaging of live cells under a fluorescence microscope. This study synthesized LbL microcapsules consisting of $(PAH/PSS)_6$/MNPs. Breast cancer cells were incubated with these layer-by-layer capsules, including magnetic nanoparticles, and cell viability was assessed using the MTT and

calcein-AM assays. The results provide insights into the biocompatibility of MNP LbL capsules against breast cancer cells.

Methods

Materials: MDA-MB-231 were purchased from the American Type Culture Collection (ATCC). Ferrofluid iron oxide nanoparticle kit were purchased from Flinn Scientific. Growth mediums and assay kits, including fetal bovine serum (FBS), high glucose DMEM, Trypsin-EDTA solution, antibiotics, MTT assay, LIVE/DEAD assay, were all purchased from Thermofisher.

Cell culture, passage, and freezing of breast cancer cell line

MDA-MB-231 cells were cultured in a medium containing F-12K/DMEM (1:1), 10% FBS, and 1% antibiotics. Similarly, MCF7 cells were cultured in culture-treated flasks using a medium composed of DMEM, 10% FBS, and 1% streptomycin and penicillin antibiotics. The cells were maintained at 37°C in a humidified 5% CO_2 incubator, with media changes occurring every 48 hours. Upon reaching 80% confluence, the cells underwent detachment using trypsin/EDTA solution and were subsequently suspended in fresh media. Cell seeding involved placing 5×10^4 cells per well in cell culture-treated 96-well plates.

For cell passage, the medium was first removed and discarded, followed by washing the dish with 5 ml of PBS twice. Subsequently, 2 ml of trypsin/EDTA was added for cell detachment, with an incubation period of 8 minutes at 37ºC. The cells were checked under a microscope to ensure detachment, and the duration of incubation was adjusted based on cell line and plate confluency. After confirming detachment, 8 ml of medium was added to the petri dish, with at least four times more medium than the applied trypsin/EDTA to neutralize its toxicity. The sample was then centrifuged.

In the process of cell freezing, cells from the MDA-MB-231 cell line were utilized [24]. This cell line, derived from excessive lung fluid in a middle-aged female patient with breast cancer, is a triple-negative breast cancer (TNBC) cell line lacking estrogen receptors, progesterone receptors, and human epidermal growth factor 2. Hence, it serves as a valuable model for studying TNBC cells. To initiate cellular freezing, cell confluency was checked, aiming for around eighty percent confluence. Following confluency verification, the medium was removed, and the dish was washed with phosphate-buffered saline (PBS) solution twice. A solution of trypsin/EDTA was added to the dish, and after incubation, the solution was centrifuged at 200g for five minutes.

Microcapsule Fabrication

$CaCO_3$ (Calcium Carbonate) is suspended in H_2O at a concentration of 10 mg/ml in a total volume of 10 ml. PAH and PSS are both dissolved in H_2O at a concentration of 4 mg/ml. To the suspended calcium carbonate, 1 ml of PAH is added and then placed on a shaker for 10 minutes. Afterward, the mixture is centrifuged, using Thermo Scientific Sorvall ST 40R centrifuge, for 10 minutes at 4,000 G. The supernatant is removed and discarded, leaving the pellet behind. The pellet is then washed two times by adding 10 ml of H_2O, centrifuging at 4,000 G for 10 minutes, following discarding the supernatant each time. Washing will remove any unbound PAH. Next, the pellet is resuspended in 9 ml of H2O, and 1 ml of the PSS solution is added and placed on the shaker for 10 minutes. Afterward, the mixture is centrifuged for 10 minutes at 4000 G. As in the previous steps involving the PAH, the supernatant is discarded, and the pellet is washed two times with 10 ml of H_2O each time. At this point, one bilayer of PAH/PSS has been added to the calcium carbonate. The binding of the PAH and PSS are charged-based. The carbonate has a negative charge and binds ionically to the positively charged PAH. Likewise, the negatively charged PSS will bind to the positively charged PAH [25, 26]. This process is repeated 6 times to achieve $(PAH/PSS)_6$.

Synthesis of Magnetite Nanoparticles

Magnetite, $Fe3O_4$, was prepared by reacting iron(III) chloride, $FeCl_3$, and iron(II) chloride, $FeCl_2$, in a 2:1 mole ratio with dilute ammonia, NH_3. A Ferrofluid Nanotechnology Demonstration kit from Flinn Lab was used as the source of these components. A 2 M solution of iron(II) chloride in hydrochloric acid, HCl, is prepared by

adding $FeCl_2 \bullet 4\ H_2O$ to 2 M HCl. Likewise, a 1 M solution of iron (III) chloride in HCl is prepared by adding $FeCl_3 \bullet 6\ H_2O$ to 2 M HCl. A combined solution of Fe(II)/Fe(III) is prepared by adding 1 ml of 2 M $FeCl_2$ to 4 ml of 1 M $FeCl_3$. Ammonia is added dropwise to the Fe(II)/Fe(III) to form a brownish-black precipitate, which is Magnetite. This reaction is an oxidation reaction in which the ammonia provides hydroxide ions, OH-, which will facilitate the oxidation and reduction of iron cations and produce the Fe_3O_4 oxide with the loss of water molecules. This is represented by the following equation:

$$2Fe^{3+}(aq) + Fe^{2+}(aq) + 8OH\text{-}(aq) \longrightarrow Fe_3O_4(s) + 4H_2O(l)$$

The Magnetite particles are collected and kept in water in the refrigerator until their incorporation into the LBL capsules [24]. The MNPs solution is added to the $(PAH/PSS)_6$ capsules suspension.

MTT assay to determine the viability of cells

Cell were seeded (5×10^4 cells/well) in cell culture treated 96 wells plates. After 24 hours, magnetic nanoparticle microcapsule solution was added to each well, and plates were incubated overnight. Next day, wells were aspirated and 100 µl fresh media and 10 µl MTT assay reagent (3-(4,5-dimethylthiazol-2-yl)-2,5-diphenyl-2H-tetrazolium bromide) was added to each well. Cells were incubated for 3 hours in the incubator, and then 100 µl detergent reagent was added to each well, and plates were kept for 2 hours in the dark at room temperature. The absorbance was read by the plate reader (Synergy2, Biotek, USA) at 570 nm.

LIVE-DEAD viability/Cytotoxicity assay

The LIVE-DEAD assay was conducted using the LIVE/DEAD Viability/Cytotoxicity Kit, adhering to the manufacturer's instructions. Briefly, cells were incubated with a combination of calcein-AM and ethidium homodimer-1 for 30 minutes at room temperature. After incubation, the cells were imaged with a fluorescence microscope. Live cells exhibited green fluorescence due to calcein-AM, while dead cells showed red fluorescence from ethidium homodimer-1. To quantify and visualize the fluorescence signals of live and dead cells, a microplate reader equipped with green and red filter cubes was used.

Scanning Electron Microscopy imaging of nanoparticles and microcapsules

Scanning electron microscopy was used to determine the morphology, size, and dimension of the MNP/LbL capsules. For collecting the samples, a small portion of the solution was applied on a clean-washed silicone surface and incubated for 1 hr. The excess liquid was taken, followed by two rinses. The surface was then left to air-dry overnight in preparation for imaging. Images were collected with a scanning electron microscope FEI Quanta 200 ESEM.

Results and Discussion

LBL capsules were created through a sequential process of introducing poly(allylamine hydrochloride) (PAH) and polystyrene sulfonate (PSS) to the calcium carbonate core. Due to the negative charge of carbonate in calcium calcium carbonate, the initial layer applied is PAH, which possesses a net positive charge. Following agitation on a shaker, centrifugation, and thorough washing to eliminate excess unbound PAH, the subsequent layer of PSS, featuring a net negative charge, is added to form a single bilayer. This bilayer addition process is iterated six times to achieve capsules with a $(PAH/PSS)_6$ structure.

As depicted in Figure 1A, a solitary bilayer on the capsules exhibits a spherical form and is notably smaller in size. During real-time microscopic observation, the capsules display dynamic movement attributed to evenly distributed repelling charges on their surface. Notably, in contrast, as illustrated in Figure 1B, capsules with six completed bilayers assume irregular shapes and tend to aggregate in solution. This suggests that the introduction of PAH and PSS, coupled with the incorporation of magnetite, introduces a level of variability, resulting in outer surfaces with non-uniform charge distributions (Figure 1C). Consequently, based on our observations, there appears to be a limitation on the successful addition of bilayers to achieve a functional capsule. In our study, we opted for six bilayers.

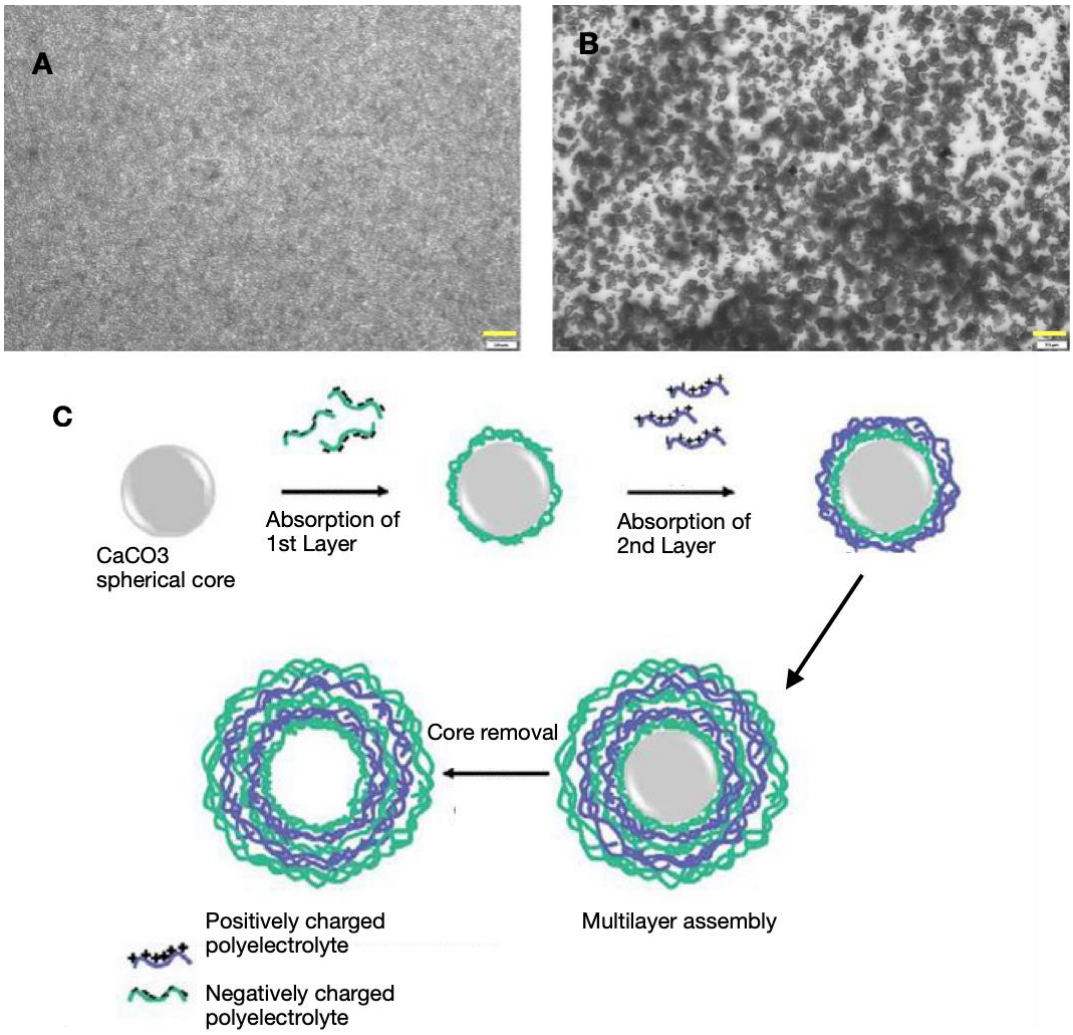

Fig. 1. A: Capsules after a single bilayer addition of PAH/PSS to the calcium carbonate core. B: completed capsules of six bilayers $(PAH/PSS)_4/(PAH/MNPs)_5/(PAH/PSS)$, containing Fe_3O_4 in the fifth layer. Completed capsules appear to lose their perfectly spherical shape and clump together in high concentrations (Scale bar 20 µm). C: Schematic image of LbL capsule assembly.

Utilizing a kit supplied by Flinn Scientific, magnetite was synthesized and stored at 4°C in an aqueous solution to prevent oxidation. In the production of capsules, magnetite replaced polystyrene sulfonate (PSS) in the fifth bilayer. A subsequent sixth bilayer, consisting of alternating PAH and PSS, was added to sandwich the magnetite between capsule layers. When observing a small droplet of the capsules on a microscope slide using an inverted microscope, with a permanent magnet positioned adjacent to the droplet, the capsules exhibited migration towards the magnet. This outcome confirmed the successful integration of magnetite nanoparticles into the capsule layers. Larger magnetite particles were discernible as black fragments, either dispersed among or situated on the periphery of the capsules.

Upon the completion of the capsules, removing the core is required for subsequent compound loading. Initially, the dissolution of the calcium carbonate core was attempted using hydrochloric acid (HCl) at an initial concentration of 0.1M, added incrementally in 100 µl portions to 1 ml of capsules in an aqueous solution.

However, limited success was observed with concentrations up to 500 µl per ml of capsules in the solution. The challenge arose from the strong acidic nature of HCl, resulting in the destruction of many capsules, even at low concentrations (Figure 2). Consequently, an alternative approach was imperative to overcome this limitation.

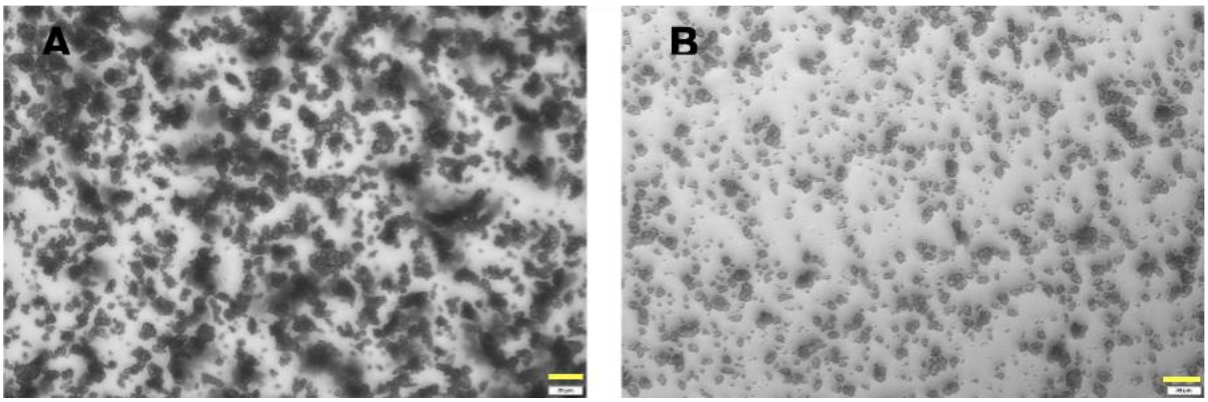

Fig. 2. Capsules with six bilayers containing MNPs in the fifth layer. A: Capsules before the addition of HCl. B: after the addition of 500 µl 0.1 M HCl. The image on the right shows the core has not been fully removed; however, a reduction in capsule numbers is observed (Scale bar 20 µm).

Ethylenediaminetetraacetic acid (EDTA) serves as a chelating agent with a notable affinity for calcium, and unlike HCl, it is less corrosive. To utilize EDTA for the removal of the calcium carbonate core, EDTA Disodium Salt Dihydrate from Fisher Scientific was dissolved in an aqueous solution at a concentration of 50 mg/ml. The removal process involved heating the crystals in a water bath at 50°C for one hour. Once all EDTA crystals were fully dissolved, capsules were introduced and subjected to incubation with EDTA. The results demonstrated a significantly improved reduction of the calcium carbonate core, as observed in Figure 3.
To examine the effects of EDTA treatment, capsules were imaged with an SEM (Scanning Electron Microscopy) microscope, the FEI Quanta 200 ESEM. As shown in Figure 4, calcium carbonate forms square-like crystals that are readily identifiable. In contrast, capsules treated with EDTA have irregular shapes as a result of calcium reduction.

MDA-MB-231 breast cancer cells were exposed to varying quantities of EDTA-treated capsules to evaluate the inherent toxicity of the capsules. The results of the MTT assay, presented in Figure 5, play a pivotal role in determining the optimal concentrations of capsules for delivering a potent cancer-killing compound, ensuring the capsules remain non-toxic. The depicted images in Figure 5 suggest that adding 20 µl of capsule suspension (containing 14,000 capsules) to 100 µl of cell culture suspension preserves 90% cell viability. Notably, reduced cell viability at higher concentrations could be attributed to factors such as the polymer nature (synthetic or biopolymers), competition for surface adhesion between cells and capsules, and the intracellular entry of capsules inside the cells.

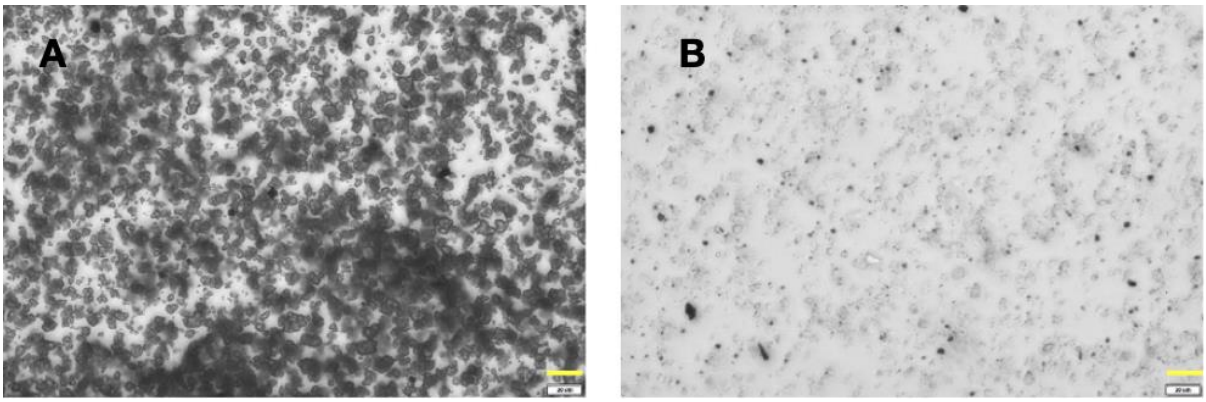

Fig. 3. A: Capsules $(PAH/PSS)_4$/MNPs prepared on $CaCO_3$ cores A. B: Hollow capsules $(PAH/PSS)_4$/MNPs after removing the $CaCO_3$ core with EDTA at a concentration of 50 mg/ml (Scale bar 20 µm).

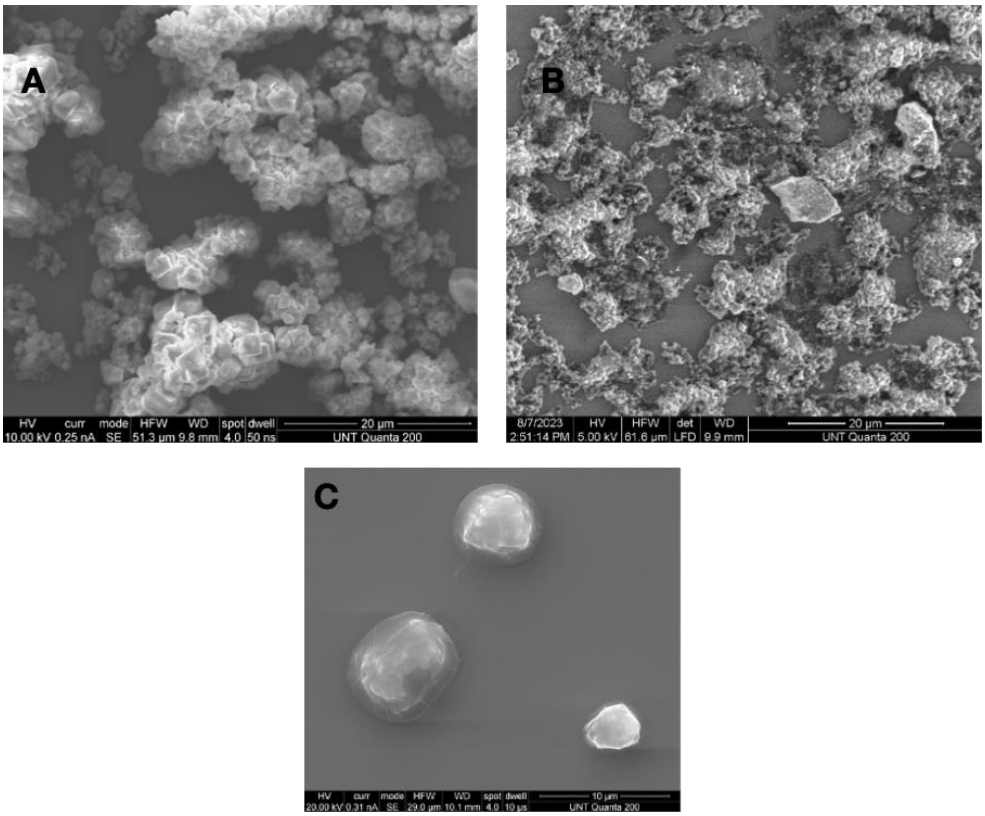

Fig. 4. SEM image of A: Capsules $(PAH/PSS)_6$/MNPs prepared on $CaCO_3$ cores; B, C: Hollow capsules treated with EDTA.

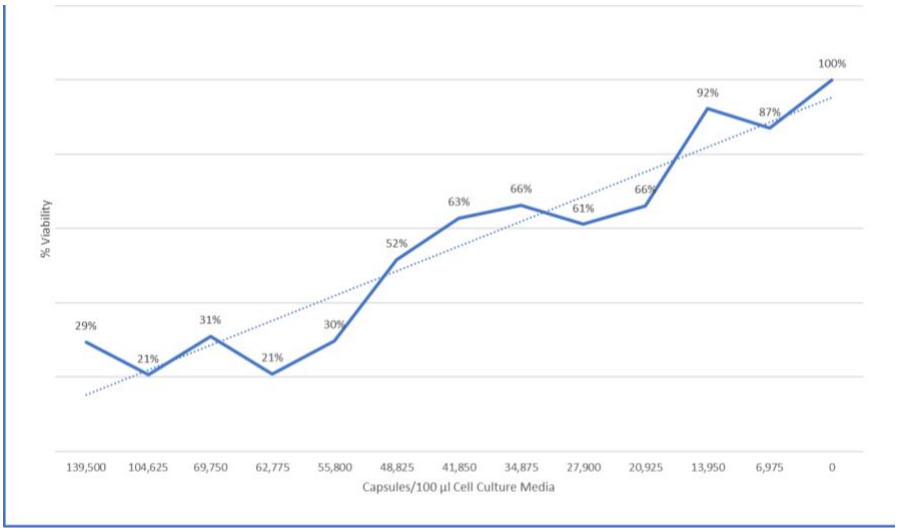

Fig. 5. MTT assay plots the viability of different amounts of capsules vs. the viability of the cells.

The LIVE-DEAD of the control cells without capsules shows that most cells are alive having green fluorescence while only few cells are displaying red fluorescence indicating being dead. The capsules at optimal concertation were exposed to cells, and Live/dead cells were analyzed. At an optimal concentration, most cells were stained green indicating being alive and few dead cells were observed (Figure 6).

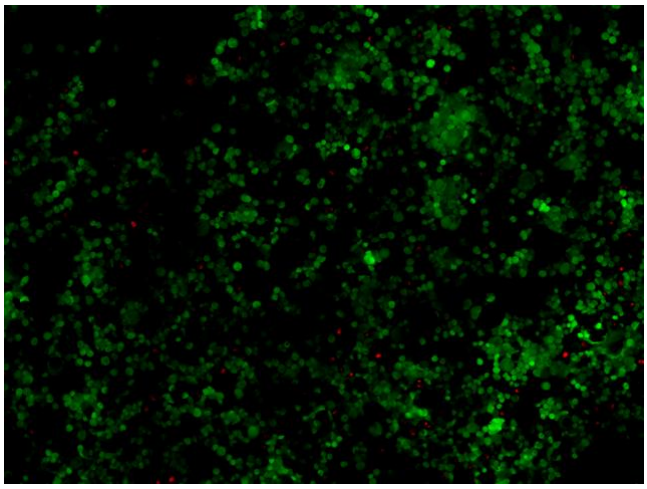

Fig. 6. Fluorescence image of LIVE-DEAD cell assay of breast cancer cells (Live cells convert calcein AM to green, fluorescent calcein, while dead cells are stained with red fluorescent ethidium homodimer-1.

Conclusion

In conclusion, this investigation was focused on evaluating the influence of drug carriers (PAH/PSS) MNP capsules on the viability of MDA-MB-231 breast cancer cells. Characterization of the capsules was conducted using SEM and bright-field microscopy, confirming successful synthesis as the capsules/MNPs demonstrated responsiveness to an external magnetic field. Utilizing the EDTA successfully removed the core with higher efficacy compared to HCl. Subsequent experimentation involved the introduction of various concentrations of capsules/MNPs to cells, with cell viability assessed through the tetrazolium-based MTT assay for quantitative measurements and the calcein-AM assay (Live-Dead) for real-time visualization of live and dead cells. The

key finding indicated that the addition of 20 µl of capsule suspension (containing 14,000 capsules) to 100 µl of cell culture suspension preserved 90% cell viability. One of the limitations of LbL capsules is changes in pH, temperature, and mechanical forces encountered in vivo, which may affect the integrity and performance of the capsules, potentially leading to premature drug release, aggregation, or clearance from the body. The efficiency, yield, and size of layer-by-layer capsules are influenced by factors such as the properties of the polyelectrolytes used, pH and ionic strength, and the characteristics of the colloidal template. Optimizing these factors allows for precise control over capsule formation, leading to tailored structures with desired properties for applications in drug delivery, sensing, and controlled release systems. This outcome suggests a viable concentration of capsules for delivering compounds to cancer cells without inducing toxicity to normal cells. In summary, the study underscores the potential of the synthesized capsules as effective drug carriers for targeted cancer therapy.

Acknowledgments We thank The Micro Nano Technology Education Center of Pasadena City College for helping initiate this collaboration and for ongoing support. We also acknowledge support from the National Science Foundation, NSF 2000281 and NSF 1720625, and National Institutes of Health grants U24 EB028887, R01 GM122424, and R16GM150848.

Disclosures
The authors declare no conflicts of interest.

References

[1] E. Garbayo, S. Pascual-Gil, C. Rodríguez-Nogales, L. Saludas, A. Estella-Hermoso de Mendoza, and M. J. Blanco-Prieto, "Nanomedicine and drug delivery systems in cancer and regenerative medicine," WIREs Nanomedicine and Nanobiotechnology, vol. 12, no. 5, Sep. 2020, doi: 10.1002/wnan.1637.

[2] A. Sarode, A. Annapragada, J. Guo, and S. Mitragotri, "Layered self-assemblies for controlled drug delivery: A translational overview,"Biomaterials, vol. 242, p. 119929, Jun. 2020, doi: 10.1016/j.biomaterials.2020.119929.

[3] K. Katagiri, M. Nakamura, and K. Koumoto, "Magnetoresponsive Smart Capsules Formed with Polyelectrolytes, Lipid Bilayers and Magnetic Nanoparticles," ACS Appl Mater Interfaces, vol. 2, no. 3, pp. 768–773, Mar. 2010, doi: 10.1021/am900784a.

[4] J. Dobson, "Magnetic nanoparticles for drug delivery," Drug Development Research, vol. 67, no. 1. pp. 55–60, Jan. 2006. doi: 10.1002/ddr.20067.

[5] A. Ali et al., "Review on Recent Progress in Magnetic Nanoparticles: Synthesis, Characterization, and Diverse Applications," Front Chem, vol. 9, Jul. 2021, doi: 10.3389/fchem.2021.629054.

[6] J. Kudr et al., "Magnetic Nanoparticles: From Design and Synthesis to Real World Applications," Nanomaterials, vol. 7, no. 9, p. 243, Aug. 2017, doi: 10.3390/nano7090243.

[7] K. Katagiri, M. Nakamura, and K. Koumoto, "Magnetoresponsive Smart Capsules Formed with Polyelectrolytes, Lipid Bilayers and Magnetic Nanoparticles," ACS Appl Mater Interfaces, vol. 2, no. 3, pp. 768–773, Mar. 2010, doi: 10.1021/am900784a.

[8] L. Xu et al., "Electrostatically Assembled Multilayered Films of Biopolymer Enhanced Nanocapsules for on-Demand Drug Release," ACS Appl Bio Mater, vol. 2, no. 8, pp. 3429–3438, Aug. 2019, doi: 10.1021/acsabm.9b00381.

[9] W. Tong, X. Song, and C. Gao, “Layer-by-layer assembly of microcapsules and their biomedical applications,” Chem Soc Rev, vol. 41, no. 18, p. 6103, 2012, doi: 10.1039/c2cs35088b.

[10] N. M. Elbaz, A. Owen, S. Rannard, and T. O. McDonald, “Controlled synthesis of calcium carbonate nanoparticles and stimuli-responsive multi-layered nanocapsules for oral drug delivery,” Int J Pharm, vol. 574, p. 118866, Jan. 2020, doi: 10.1016/j.ijpharm.2019.118866.

[11] R. Kurapati, T. W. Groth, and A. M. Raichur, “Recent Developments in Layer-by-Layer Technique for Drug Delivery Applications,” ACS Appl Bio Mater, vol. 2, no. 12, pp. 5512–5527, Dec. 2019, doi: 10.1021/acsabm.9b00703.

[12] E. V. Lengert et al., “Nanoparticles in Polyelectrolyte Multilayer Layer-by-Layer (LbL) Films and Capsules—Key Enabling Components of Hybrid Coatings,” Coatings, vol. 10, no. 11, p. 1131, Nov. 2020, doi: 10.3390/coatings10111131.

[13] S. A. Sukhishvili, “Responsive polymer films and capsules via layer-by-layer assembly,” Curr Opin Colloid Interface Sci, vol. 10, no. 1–2, pp. 37–44, Aug. 2005, doi: 10.1016/j.cocis.2005.05.001.

[14] F. Sousa, O. Kreft, G. B. Sukhorukov, H. Möhwald, and V. Kokol, “Biocatalytic response of multi-layer assembled collagen/hyaluronic acid nanoengineered capsules,” J Microencapsul, vol. 31, no. 3, pp. 270–276, May 2014, doi: 10.3109/02652048.2013.834995.

[15] A. L. Becker, A. P. R. Johnston, and F. Caruso, “Layer-By-Layer-Assembled Capsules and Films for Therapeutic Delivery,” Small, vol. 6, no. 17, Sep. 2010, doi: 10.1002/smll.201000379.

[16] C. Zheng, Y. Ding, X. Liu, Y. Wu, and L. Ge, “Highly magneto-responsive multilayer microcapsules for controlled release of insulin,” Int J Pharm, vol. 475, no. 1–2, pp. 17–24, Nov. 2014, doi: 10.1016/J.IJPHARM.2014.08.042.

[17] C. E. Stavarache and L. Paniwnyk, “Controlled rupture of magnetic LbL polyelectrolyte capsules and subsequent release of contents employing high intensity focused ultrasound,” J Drug Deliv Sci Technol, vol. 45, pp. 60–69, Jun. 2018, doi: 10.1016/j.jddst.2018.02.011.

[18] M. Nakamura, K. Katagiri, and K. Koumoto, “Preparation of hybrid hollow capsules formed with Fe3O4 and polyelectrolytes via the layer-by-layer assembly and the aqueous solution process,” J Colloid Interface Sci, vol. 341, no. 1, pp. 64–68, Jan. 2010, doi: 10.1016/j.jcis.2009.09.014.

[19] O. L. Herrera, E. Parigi, N. Habibi, L. Pastorino, F. C. Soumetz, and C. Ruggiero, “Development of nanostructured magnetic capsules by means of the layer by layer technique,” in 2010 Annual International Conference of the IEEE Engineering in Medicine and Biology, IEEE, Aug. 2010, pp. 6477–6480. doi: 10.1109/IEMBS.2010.5627353.

[20] F. Ridi, M. Bonini, and P. Baglioni, “Magneto-responsive nanocomposites: Preparation and integration of magnetic nanoparticles into films, capsules, and gels,” Advances in Colloid and Interface Science, vol. 207, no. 1. Elsevier B.V., pp. 3–13, 2014. doi: 10.1016/j.cis.2013.09.006.

[21] M. V. Zyuzin, A. S. Timin, and G. B. Sukhorukov, “Multilayer Capsules Inside Biological Systems: State-of-the-Art and Open Challenges,” Langmuir, vol. 35, no. 13, pp. 4747–4762, Apr. 2019, doi: 10.1021/acs.langmuir.8b04280.

[22] J. van Meerloo, G. J. L. Kaspers, and J. Cloos, “Cell Sensitivity Assays: The MTT Assay,” Cancer cell culture, vol. 731, pp. 237–245, 2011.

[23] T. Riss, A. Niles, R. Moravec, N. Karassina, and J. Vidugiriene, Cytotoxicity Assays: In Vitro Methods to Measure Dead Cells. 2004.

[24] K. A. Akshata Desai, “Triple Negative Breast Cancer – An Overview,” Hereditary Genetics, 2012, doi: 10.4172/2161-1041.S2-001.

[25] K. Podgórna and K. Szczepanowicz, “Synthesis of polyelectrolyte nanocapsules with iron oxide (Fe 3 O 4) nanoparticles for magnetic targeting,” Colloids Surf A Physicochem Eng Asp, vol. 505, pp. 132–137, Sep. 2016, doi: 10.1016/j.colsurfa.2016.02.017.

[26] J.-P. Chapel and J.-F. Berret, “Versatile electrostatic assembly of nanoparticles and polyelectrolytes: Coating, clustering and layer-by-layer processes,” Curr Opin Colloid Interface Sci, vol. 17, no. 2, pp. 97–105, Apr. 2012, doi: 10.1016/j.cocis.2011.08.009.